Ruby fluorescence pressure scale: Revisited*

Liu Lei(柳 雷), Bi Yan(毕 延)†, and Xu Ji-An(徐济安)

National Key Laboratory of Shock Wave and Detonation Physics, Institute of Fluid Physics, China Academy Of Engineering Physics, Mianyang 621900, *China*

(Received 11 October 2012; revised manuscript received 5 December 2012)

Effect of non-hydrostatic stress on X-ray diffraction in a diamond anvil cell (DAC) is studied. The pressure gradient in the sample chamber leads to the broadening of the diffraction peaks, which increase with the *hkl* index of the crystal. It is found that the difference between the determined d-spacing compressive ratio d/d_0 and the real d-spacing compressive ratio d_r/d_0 is determined by the yield stress of the pressure transmitting media (if used) and the shear modulus of the sample. On the basis of the corrected experiment data of Mao *et al.* (MXB86), which was used to calibrate the most widely used ruby fluorescence scale, a new relationship of ruby fluorescence pressure scale is corrected, i.e., $P = (1904/9.827)[(1+\Delta\lambda/\lambda_0)^{9.827} - 1]$.

Keywords: non-hydrostatic stress, ruby fluorescence pressure scale, diamond anvil cell

PACS: 62.20.D–, 64.30.Ef, 07.35.+k **DOI:** 10.1088/1674-1056/22/5/056201

1. Introduction

The development of the ruby fluorescence pressure scale has promoted the rapid growth of high-pressure physics, chemistry, and geophysics with the diamond anvil cell (DAC) technology. It provides a simple and quick method for determining pressure, and a series of high-pressure experiments (high-pressure Raman, Brillouin, electrical, magnetism measurements, and so on) can be carried out in various laboratories. Forty years have passed since Forman[1] proposed the shift of a ruby R_1 line as a pressure gauge. The first widely used non-hydrostatic ruby pressure scale (MBSS78) was calibrated by Mao *et al.*[2] to about 100 GPa on the basis of 300-K isotherms of Cu, Mo, Pd, and Ag derived from shock wave Hogoniot data. Later, Mao and co-workers[3] improved the MBSS78 scale by determining the volumes of Cu and Ag in argon pressure transmitting media (PTM) and established the most widely used quasi-hydrostatic pressure gauge up to now, named MXB86. Since then, a number of revisions[4–12] have been made, as summarized in Table 1. Four important revisions are worthwhile mentioning here.

ZMH00[5] The MgO primary pressure scale was established by combining the Brillouin and X-ray diffraction measurement after Xu and Huang's proposal.[13] The ZMH00 scale was calibrated based on the MgO primary pressure scale. This work is important because this calibration is not on the basis of shock wave reduced isotherms (SWRIs). Therefore, it has no relation with the uncertainties in shock wave measurement, strength of sample, assumptions of the volume dependence of the Grüneisen parameter, and the one-dimensional nature of shock waves.[5]

H03[6] Calibrated on the basis of the ultrasonic data of diamond and Ta at low pressure, the functional form III affords more flexibility at high pressure. However, it is too complicated at lower pressure ($<$ 200 GPa), where the functional form I is adequate.[9,14,15]

Table 1. Ruby pressure scales. There are four functional forms to describe the ruby R_1 line shift with pressure: (I) $P = (A/B)[(1+\Delta\lambda/\lambda_0)^B - 1]$, (II) $P = A((\lambda-\lambda_0)/\lambda_0)(1+B(\lambda-\lambda_0)/\lambda_0)$, (III) $P = A/(B+C)(\exp\{(B+C)[1-(\lambda/\lambda_0)^{-C}]/C\} - 1)$, (IV) $P = A[(\lambda-\lambda_0)/\lambda + B((\lambda-\lambda_0)/\lambda)^2]$, where λ_0 is the wavelength of R_1 line at ambient conditions ($\lambda_0 = 694.24$ nm), λ is the wavelength of R_1 line at pressure of P, and A, B, C are the fitting parameters.

Ref.	Pressure scale	Parameters
[2]	MBSS78	I: A=1904, B=5
[3]	MXB86	I: A=1904, B=7.665
[4]	AGZS87	I: A=1918, B=11.7 II: A=1892, B=6.4
[5]	ZMH00	I: A=1904, B=7.715
[6]	H03	I: A=1904, B=10.8 III: A=1820, B=14, C=7.3
[7]	DO03	I: A=1871, B=10.06
[8]	DLM04	I: A=1904, B=9.5
[9], [10]	CNSS05	I: A=1876, B=10.71 IV: A=1798, B=8.57
[11]	DO07	II: A=1884, B=5.5
[12]	DTLM08	I: A=1920, B=9.61

DLM04[8] Dorogokupets regarded this as a "revolutionary" work.[11] This work revealed the systemic errors in SWRIs and tried to remove the errors by a sophisticated mathematic procedure in order to calibrate a new ruby pressure scale. The ruby pressure scale calibrated by this method is dependent on the standard materials selected. The discrepancy between DLM04 and DTLM08[12] reaches 1.3 GPa at 120 GPa, just because different standard materials were selected in these two pressure scales. The "fan" curves in

*Project supported by the Defense Industrial Technology Development Program of China (Grant No. B1520110001), the National Natural Science Foundation of China (Grant No. 10874158), and the Project of China Academy of Engineering Physics (Grant Nos. 2010A0101001 and 2008A0101001).

†Corresponding author. E-mail: biyan_cn@yahoo.com.cn

© 2013 Chinese Physical Society and IOP Publishing Ltd

Fig. 3(b) of Ref. [8] may indicate intrinsic property-dependent errors of shock wave data reduce procedure, which is not included in the systemic error. This material-dependent error needs further study.

CNSS05[9] The ruby pressure scale has been carefully calibrated based on SWRIs with thermal and material strength corrections.

Through checking the calibration process of a ruby pressure scale from an experimental aspect, the following four effects must be considered carefully in order to achieve an accurate ruby pressure scale.

Uncertainty in SWRIs Up to now, SWRIs are the basis of a ruby fluorescence pressure scale because other primary pressure scales are still absent at high pressures. The precision of SWRIs determines the precision of the ruby pressure scale.

Pressure gradient The pressure gradient exists at high pressures even when the PTM has been used.[16–18] The standard material and ruby chips need to be located as near as possible to avoid the effect of any pressure gradient.

Strength effect The strength of the PTM leads to a stress along the axis direction, which is larger than that along the radial direction in a DAC. This effect makes the measured d-spacings of standard materials larger than those at the corresponding hydrostatic pressure, and an un-neglected pressure error is unavoidable.[19] This effect is discussed in detail in Section 2.

Mismatch in strengths and elastic properties The pressure in the sample materials and ruby would be different from each other because of the stress concentration in incompressible materials, arising from their mismatch on strengths and elastic properties.[17,20–23] Among the standard materials, W is considered as the best material which matches the strength and elastic properties of ruby.[17]

Previous efforts to revise the ruby pressure scale normally were focused on the correction of SWRIs and the search for more accurate pressure standards. Careful checks on DAC experiments themselves are still lacking. In this paper, the effect of non-hydrostatic stress on X-ray diffraction in a DAC is studied. The strength effect of the PTM in Mao's results is corrected and a new ruby pressure scale is calibrated.

2. Non-hydrostatic pressure effects in X-ray diffraction determination

2.1. Stress state in the sample chamber of a DAC

The stress in the sample chamber in a DAC can be classified into two types: macroscopic stress and microscopic stress. The microscopic stress is the deviatoric stress field throughout the sample, which varies from grain to grain. The effect of this microscopic deviatoric stress field would be the broadening on the diffraction lines.[14] The macroscopic stress produced in a sample has been sketched in Fig. 1. The macroscopic non-hydrostaticity in the sample chamber of a DAC includes two situations: the pressure gradient (pressure varies with positions) and the differential stress (pressure varies with directions). As shown in Fig. 1, there is pressure distribution along the radial direction in the sample zone where X-ray covered, then the X-ray diffraction signal from this region involve the properties of materials under different pressures. This may cause the broadening of the diffraction peaks. Differential stress means that σ_z and σ_x (or σ_y) are different throughout the sample chamber. A crystal lattice influenced by differential stress deforms in the following way: the lattice planes lying perpendicular to the principle stress direction σ_z are more compressed compared with that in a hydrostatic case, whereas the planes lying parallel to σ_z expand more obviously due to Poisson's effect. In the conventional diffraction geometry, the incident X-ray beam is nearly parallel to the stress direction σ_z. It follows that the X-ray beam is diffracted only by the lattice planes lying nearly parallel to σ_z, and accordingly the observed interplanar spacing becomes larger than the hydrostatic case. The expansion of the interplanar spacing causes a shift of the diffraction peak to a lower scattering angle.

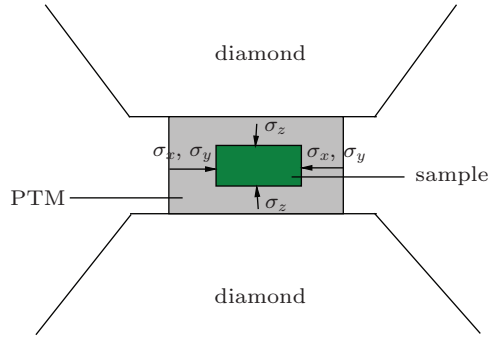


Fig. 1. (color online) Sketch map of the macroscopic stress born on the sample.

2.2. Pressure gradient

The broadening of diffraction lines can be described as follows (see Appendix A):

$$\begin{aligned}\Delta\theta &= -\frac{\lambda}{6d\sqrt{1-\lambda^2/4d}}\frac{Y}{h}\frac{R}{K}\\ &= -\frac{\lambda}{6d\sqrt{1-\lambda^2/4d}}\frac{\mathrm{d}P(r)}{\mathrm{d}r}\frac{R}{K},\end{aligned} \tag{1}$$

where θ, λ, Y, h, R, K, r, and $P(r)$ are the diffraction angle, X-ray wavelength, yield strength, thickness, X-ray beam size, bulk modulus, radial distance, and pressure distribution. Equation (1) indicates that the yield strength of the sample (or PTM if PTM is used), the bulk modulus of the sample, the thickness of the sample, and the size of the X-ray beam all contribute to the broadening of the diffraction lines. The maximum broadening occurs when the maximum pressure

gradient appears. Jing *et al.*[25] determined the pressure distribution in Mo along the radial direction at high pressures. Take their data as an example, we calculated the broadening width of the diffraction line according to Eq. (1) at 21 GPa (peak pressure). Suppose that the X-ray beam size is 10 μm and the wavelength is 0.6199 Å (the wavelength used at 4W2 High-Pressure Station of Beijing Synchrotron Facility), we calculated the differential strain in Mo. The results have been illustrated in Fig. 2. In the center of the sample chamber, the pressure reaches the maximal value and its radial distance derivative is zero, so no differential strain appears. It is worth mentioning that the maximal differential strain appears at ±80 μm. We must avoid loading the sample at these positions. The broadening widths of diffraction lines of Mo were also calculated and shown in Fig. 3.

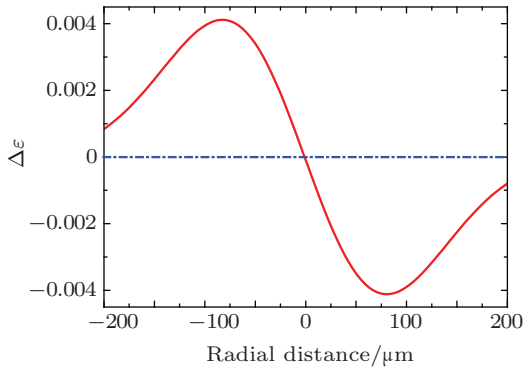


Fig. 2. (color online) Variation of the differential strain of Mo with the radial distance.

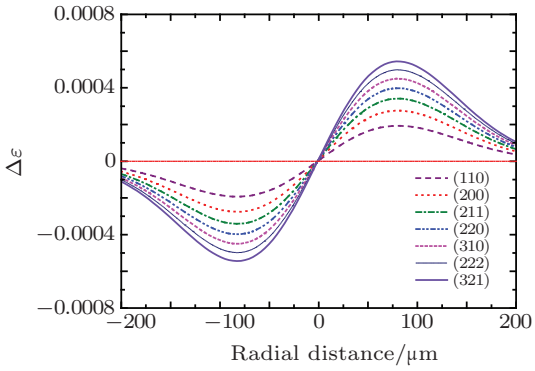


Fig. 3. (color online) Broadening widths of diffraction lines of Mo at 21 GPa as a function of the radial distance.

The results demonstrate that the broadening widths of diffraction lines increase with decreasing d-spacing. In angle dispersive X-ray diffraction (ADXD) experiments, the broadening widths of diffraction lines increase with increasing diffraction angle 2θ. In fact, the maximum pressure gradient strongly depends on the function of the pressure distribution. Kimura[24] proposed an exponential function to describe the pressure distribution, while Jing *et al.*[25] used the cubic polynomial. Jing *et al.* examined different functions and found that minimum residual error has been obtained when using a cubic polynomial to fit the experimental data of the pressure distribution. The maximal broadening width appears at about ±85 μm when using cubic polynomial. This result was very close to our result by using a Gaussian function.

2.3. Differential stress

Figure 1 is the sketch map of the macroscopic stress produced in the sample. We assume that the strains resulting from the stress are small, the materials are in their elastic region. According to Hook's Law, the strains in x, y, and z directions are given by

$$\varepsilon_x = \frac{1}{E_{\text{sample}}}(\sigma_x - \nu_{\text{sample}}(\sigma_y + \sigma_z)), \tag{2}$$

$$\varepsilon_z = \frac{1}{E_{\text{sample}}}(\sigma_z - \nu_{\text{sample}}(\sigma_y + \sigma_x)), \tag{3}$$

where E_{sample} and ν_{sample} are Young's modulus and the Poisson ratio of the sample, respectively. The difference of the strains in x and z directions are

$$\Delta\varepsilon = \varepsilon_z - \varepsilon_x = \frac{1}{E_{\text{sample}}}[(\sigma_z - \sigma_x) + \nu_{\text{sample}}(\sigma_z - \sigma_x)]. \tag{4}$$

When the PTM was obtained, we have

$$\sigma_z - \sigma_x = t = Y_{\text{PTM}}, \tag{5}$$

where Y_{PTM} is the yield strength of the PTM, so the difference of the strains in the x and z directions can be rewritten as

$$\Delta\varepsilon = \frac{(1+\nu_{\text{sample}})Y_{\text{PTM}}}{E_{\text{sample}}}, \tag{6}$$

$$\Delta\varepsilon = \frac{Y_{\text{PTM}}}{2G_{\text{sample}}}, \tag{7}$$

where G_{sample} is the shear modulus of the sample. In the traditional axial diffraction geometry, the determined strain is very close to ε_x, as illustrated in Fig. 1. The difference between the determined strain and the true strain in the sample is given by

$$\Delta\varepsilon' = \frac{\varepsilon_x + \varepsilon_y + \varepsilon_z}{3} - \varepsilon_x = \frac{1}{3}(\varepsilon_z - \varepsilon_x) = \frac{1}{3}\Delta\varepsilon = \frac{Y_{\text{PTM}}}{6G_{\text{sample}}}. \tag{8}$$

Equation (8) indicates that $\Delta\varepsilon'$ is determined by the ratio of the yield strength of the PTM to the shear modulus of the sample: greater yield strength of the PTM and smaller shear modulus of the sample lead to larger difference between the determined strain and the true strain of the sample. For equation of state (EOS) determination, the hydrostaticity is not determined by the yield strength of the PTM only, but determined by the mechanical properties of both the PTM and the sample simultaneously. Equation (8) can be used as a criteria for the choice of various PTMs. The $\Delta\varepsilon'$ of copper, silver, platinum, molybdenum, and tungsten are calculated when Ar was used as the PTM, and the results are illustrated in Fig. 4.

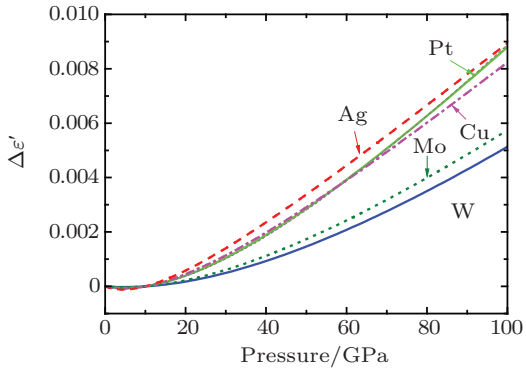


Fig. 4. (color online) Variation of $\Delta\varepsilon' = Y_{\rm Ar}/6G_{\rm sample}$ of copper, silver, platinum, molybdenum, and tungsten with pressure when Ar is used as PTM. The yield strength data of argon was taken from Ref. [26]: $Y = 0.001P^2 - 0.01P$. The values of the shear modulus of Cu, Ag, Pt, Mo, and W are taken from Refs. [27]–[30], respectively, and fitted with linear function: $G_{\rm Cu} = 47.11 + 1.35P$; $G_{\rm Ag} = 29.67 + 1.38P$; $G_{\rm Pt} = 62.75 + 1.077P$; $G_{\rm Mo} = 123.36 + 1.38P$; and $G_{\rm W} = 163.06 + 1.29P$.

3. Ruby pressure scale

The measured d/d_0 in Mao *et al.*'s DAC experiments with the conventional diffraction geometry is nearly equal to d_x/d_0, while the real values of d-spacing compressive ratio $d_{\rm r}/d_0$ is $(2d_x + d_z)/3d_0$. According to the result in Section 2.3, we have

$$\frac{d_{\rm r}}{d_0} = \frac{2d_x + d_z}{3d_0} = \frac{d_x}{d_0} - \frac{1}{3}\frac{Y_{\rm PTM}}{6G_{\rm sample}}. \tag{9}$$

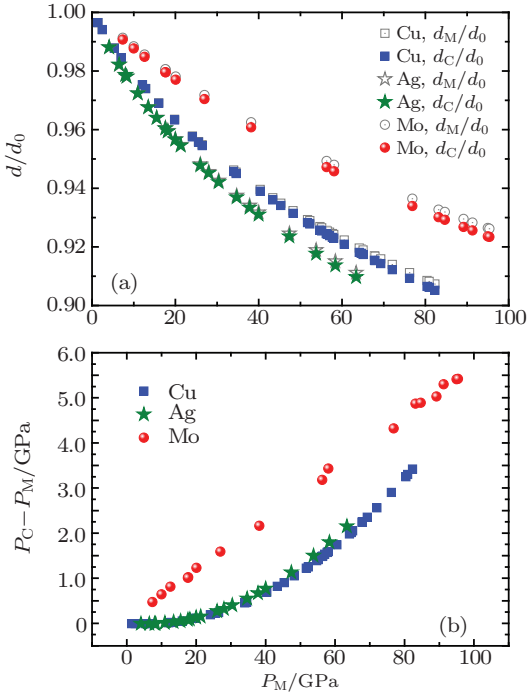


Fig. 5. (color online) (a) Measured ($d_{\rm M}/d_0$) and corrected ($d_{\rm C}/d_0$) compressive ratios of d-spacings. (b) Difference between the corrected pressure ($P_{\rm C}$) and the measured pressure ($P_{\rm M}$).

The corrected $d_{\rm r}/d_0$ results of Mao *et al.*'s d/d_0 based on Eq. (9) , and the recalculated pressure on the basis of Carter's SWRIs,[31] which were used in Mao *et al.*'s work, are shown in Fig. 5. When calibrating the MXB86 pressure scale, Cu and Ag were compressed in argon. The ratio of $Y_{\rm argon}/6G_{\rm sample}$ of Cu and Ag are illustrated in Fig. 4. Mo was compressed in methanol–ethanol (ME) solution (volume ratio 4:1). However, the yield strength data of ME is lacking, and so the yield strength of Mo determined by radial X-ray diffraction[30] was used instead.

The new calibrated ruby pressure scales are illustrated in Fig. 6. The recalibrated scale based on corrected Cu and Ag data gives $A = 1904$ (constant during the fitting procedure), and $B = 9.827$ (P_1 scale) of functional form I. Fitting the corrected results of Mo with functional form I, we obtain $A = 1904$, and $B = 8.761$ (P_2 scale). The difference between P_1 and other pressure scales is illustrated in Fig. 7. The P_1 scale agrees well with DLM04, CNSS05, DO07, and DTLM08 scales below 100 GPa.

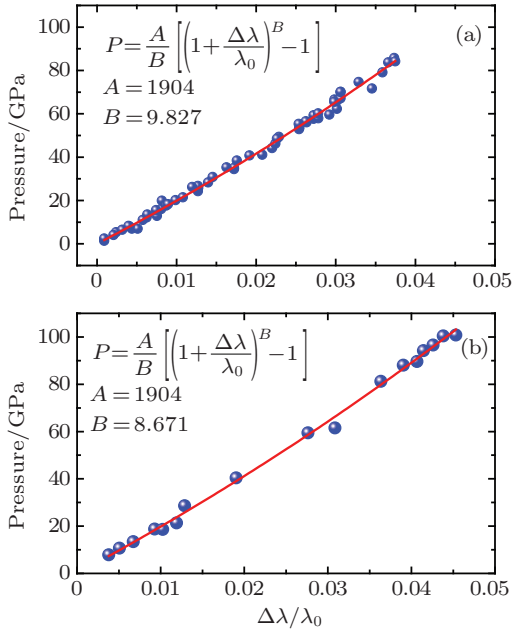


Fig. 6. (color online) Recalibrated ruby pressure scales on the basis of the corrected data for (a) Cu&Ag in argon, and (b) Mo in 4:1 ME solution.

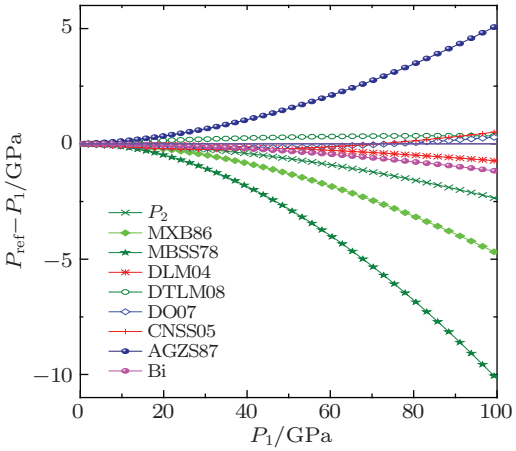


Fig. 7. (color online) Discrepancies between P_1 and other pressure scales. Bi represents the pressure scale calibrated by Bi *et al.*[32]

The P_2 scale gives lower pressure than P_1 scale. This discrepancy may arise from the uncertainty of the values of the strength and shear modulus, which are extrapolated to higher pressures.

4. Conclusions

The potential uncertainties in the MBSS78 and MXB86 pressure scale arising from the DAC experiments themselves are checked carefully. The effect of the non-hydrostatic stress environment in X-ray diffraction is studied. It is found that the determined d-spacing compressive ratio d/d_0 is larger than the value of real d-spacing compressive ratio d_r/d_0. This correction has been performed by Mao *et al*. and a new ruby pressure scale ($A = 1904$, $B = 9.827$) is proposed.

Acknowledgements

The authors thank Dr. Song Zhen-Fei for useful discussion.

Appendix A

The following equation can be derived from the definition of bulk modulus in the elastic region of materials

$$\frac{\Delta V}{V_0} = -\frac{P}{K}, \tag{A1}$$

where V_0, P, and K are the volume at ambient pressure, pressure, and bulk modulus, respectively. Then, the differential stain $\Delta\varepsilon$ at different pressures can be written as follows:

$$\Delta\varepsilon = -\frac{\Delta P}{K}. \tag{A2}$$

If the pressure distribution along the radial direction of sample chamber is $P(r)$, equation (2) can be rewritten as

$$\Delta\varepsilon = -\frac{\mathrm{d}P(r)}{\mathrm{d}r}\frac{R}{K} = \frac{t}{h}\frac{R}{K} = \frac{Y}{h}\frac{R}{K}, \tag{A3}$$

where R is the diameter of X-ray beam, t is the differential stress, which is the difference between σ_z and σ_x (or σ_y), Y is the yield strength of the sample, and h is the thickness of the gasket. Differential stress t equals the yield strength of the sample in Von Mises yield condition. According to Bragg's law, the broadening of diffraction line $\Delta\theta$ caused by the uncertainty of d-spacing Δd is given by

$$\Delta\theta = -\frac{\lambda}{2d\sqrt{1-\lambda^2/(4d^2)}}\frac{\Delta d}{d}. \tag{A4}$$

The relationship between the differential stain $\Delta\varepsilon$ and the uncertainty of d-spacing Δd is

$$\Delta\varepsilon(r) = 3\frac{\Delta d}{d}. \tag{A5}$$

Using Eqs. (A3) and (A5), equation (A4) can be rewritten as follows:

$$\begin{aligned}\Delta\theta &= -\frac{\lambda}{6d\sqrt{1-\lambda^2/4d}}\frac{Y}{h}\frac{R}{K} \\ &= -\frac{\lambda}{6d\sqrt{1-\lambda^2/4d}}\frac{\mathrm{d}P(r)}{\mathrm{d}r}\frac{R}{K}.\end{aligned} \tag{A6}$$

References

[1] Forman R A, Piermarini G J, Barnett J D and Block S 1972 *Science* **176** 284
[2] Mao H K, Bell P M, Shaner J W and Steinberg D J 1978 *J. Appl. Phys.* **49** 3276
[3] Mao H K, Xu J and Bell P M 1986 *J. Geophys. Res.* **91** 4673
[4] Aleksandrov I V, Goncharov A F, Zisman A N and Stishov S M 1987 *Sov. Phys. JETP* **66** 384
[5] Zha C S, Mao H K and Hemley R J 2000 *Proc. Natl. Acad. Sci. USA* **97** 13494
[6] Holzaphel W B 2003 *J. Appl. Phys.* **93** 1813
[7] Dorogokupets P I and Oganov A R 2003 *Dokl. Earth Sci.* **391A** 854
[8] Dewaele A, Loubeyre P and Mezouar M 2004 *Phys. Rev. B* **70** 094112
[9] Chijioke A D, Nellis W J, Soldatov A and Silvera I F 2005 *J. Appl. Phys.* **98** 114905
[10] Silvera I F, Chijioke A D, Nellis W J, Soldatov A and Tempere J 2007 *Phys. Stat. Sol. (b)* **244** 460
[11] Dorogokupets P I and Oganov A R 2007 *Phys. Rev. B* **75** 024115
[12] Dewaele A, Torrent M, Loubeyre P and Mezouar M 2008 *Phys. Rev. B* **78** 104102
[13] Xu J and Huang E 1998 *J. Geo. Soc. China.* **41** 199
[14] Kunc K, Loa I and Syassen K 2003 *Phys. Rev. B* **68** 094107
[15] Kunc K, Loa I and Syassen K 2004 *High Press. Res.* **24** 101
[16] Klotz S, Chervin J C, Munsch P and Marchand G L 2009 *J. Phys. D: Appl. Phys.* **42** 075413
[17] Tempere J and Silvera I F 2011 *J. Appl. Phys.* **110** 113523
[18] Wang J H and He D W 2008 *Acta Phys. Sin.* **57** 3397 (in Chinese)
[19] Syassen K 2008 *High Press. Res.* **28** 75
[20] Sung C M, Goetze C and Mao H K 1977 *Rev. Sci. Instrum.* **48** 1386
[21] Duffy T S, Mao H K and Hemley R J 1995 *Phys. Rev. Lett.* **74** 1371
[22] Wang J, He D and Duffy T S 2010 *J. Appl. Phys.* **108** 063521
[23] Jing Q M, Wu Q, Liu L, Bi Y, Zhang Y, Liu S G and Xu J 2012 *Chin. Phys. B* **21** 106201
[24] Kimura H, Ast D G and Basset W A 1982 *J. Appl. Phys.* **53** 3523
[25] Jing Q M, Bi Y, Wu Q, Jing F Q, Wang Z G and Xu J A 2007 *Rev. Sci. Instrum.* **78** 073906
[26] Mao H K, Badro J, Shu J, Hemley R J and Singh A K 2006 *J. Phys.: Condens. Matter* **18** S963
[27] Daniels W B and Smith C S 1958 *Phys. Rev.* **111** 713
[28] Proupin E M and Singh A K 2007 *Phys. Rev. B* **76** 054117
[29] Katahara R W and Manghnani M H 1979 *J. Phys. F: Met. Phys.* **9** 773
[30] He D W and Duffy T S 2006 *Phys. Rev. B* **73** 134106
[31] Carter W J, Marsh S P, Fritz J N and McQueen R G 1971 *Natl. Bur. Stand. (U.S.). Spec. Publ.* **326** 147
[32] Bi Y *et al.* (to be submitted)